

Wireless Recorder for Intracranial Epileptic Seizure Monitoring

Aidan Curtis, Sophia D'Amico, Andres Gomez, Benjamin Klimko, Zhiyang Zhang

Electrical and Computer Engineering

Rice University

Houston, TX, USA

riceaxonmobile@gmail.com

I. ABSTRACT

Our team has developed a wireless neural recording system to help eliminate the issues faced by patients who undergo wired neural monitoring for epilepsy. Existing neural recording system solutions are wired and require patients to remain in the hospital for weeks at a time. This process is expensive and highly likely to cause infection and stress. A solution to this problem is to develop a wireless alternative. The device we created, in a 4x4 centimeter circuit board footprint, has a front-end interface chip that performs signal conditioning on the neural data, a wireless link to a receiver, a novel data compression algorithm, and a power management system. The final product is a form-factor system that can be implemented in test animals for experimentation purposes and is scalable to humans. It can transmit as far as 10 meters, has a battery life of approximately 20 hours, and can sample neural data at up to 1 kilohertz, with 16-bit analog-to-digital conversion. Our device's use in epilepsy treatment can decrease treatment cost, decrease hospital stay, and improve patient quality of life.

II. INTRODUCTION

Intracranial and extracranial EEG recordings have applications in clinical epilepsy treatment and neuroscience research. According to the World Health Organization, 30% of all epilepsy patients do not respond to medication to keep their seizures under control [1]. One of the most effective ways of treating these patients is to use electrocorticography (ECoG) to localize epileptogenic zones and then remove the affected area of the brain. ECoG is a procedure that uses electrodes placed directly on the exposed surface of the brain to record electrical activity from the cerebral cortex. Compared to electroencephalogram (EEG) scalp recording, ECoG achieves greater precision and sensitivity through invasive electrodes implanted through the skull [2]. There are two types of signals that can be recorded: local field potentials (LFP) and action potentials (spike data). LFP data is used to analyze the activity of many neurons in a network as a whole, whereas action potentials are used to determine the activity of individual neurons [3]. Since activations from collections of neurons change on a much larger time scale, a sampling rate of 100 Hz for EEG recordings and 1000 Hz for ECoG recordings is sufficient to capture most relevant LFP information. However,

action potential spikes are much quicker and last for a short period of time, so a sampling rate around 30 kHz is required [4].

The most commonly used system for recording neural data is tethered. Electrodes are wired from inside the brain to a stationary external source that collects the data. According to our sponsor, Dr. Nitin Tandon of UT Health's Neuroimaging and Electrophysiology Lab [5], the presence of wires in his recording process causes two main problems: 1) the patients have limited mobility throughout the duration of the data recording and must remain in the hospital for days or even weeks, and 2) the wires are a potential source of infection. An extended hospital stay is very expensive, and the cost only goes up if infection occurs. Additionally, being unable to move around for potentially weeks is detrimental to the patient's well-being. While there are a handful of commercial wireless implantations, like Medtronic's Activa system [6], they are meant for chronic implantation, while focusing on neurostimulation and therapy, rather than recording neural data to identify the affected area. Dr. Tandon currently uses Blackrock's NeuroPort Recording System [7] with his patients, which does not have the advantage of being wireless.

It would be impractical to test our invasive device prototype on human beings because of FDA regulations. Therefore, for an initial demonstration, we have designed a wireless EEG/ECoG device that can be implanted into a rat's brain. Our system design is scalable in the number of channels and bandwidth, while maintaining sufficiently low power, to enable future use in human patients. Additionally, our system would enable patient mobility, potentially reducing hospital stays and improving quality of life during the recording process. Lastly, to set our device apart from existing solutions, we implemented a unique data compression technique on our collected neural data.

III. SYSTEMS ENGINEERING

We have designed and demonstrated a compact 4x4cm prototype that will digitize and transmit data from electrode arrays in patients to a nearby data collection device. The project contains four major subsystems: (1) A power management system; (2) Front-end interface chip that performs signal

conditioning; (3) An original data compression algorithm; (4) A wireless link to a receiver.

Electrodes implanted in the brain transmit data to a chip that records EEG data on a custom-designed interface board. The chip then sends the data to a microcontroller that implements a novel compression algorithm. Next, the data is sent via proprietary RF to an external receiver, where the packets are decoded in real time and visualized. Figure 1 below shows a flow chart of our system, including a breakdown of what each subsystem does.

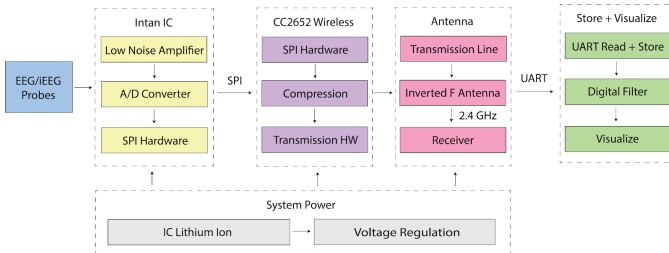


Fig. 1: System-Level Design

Electrodes connect to our data acquisition chip from Intan Technologies, where the data undergoes low pass filtering, digitization, and amplification. The data is then transferred via SPI protocol to our wireless microcontroller, which samples the data, performs compression, and transmits the data through a transmission line and an inverted F antenna. Lastly, the data is received and sent to a computer via UART where it can be read, stored, visualized and analyzed.

IV. SPECIFICATIONS

Our customer is the same as our sponsor, Dr. Tandon. He wanted for our system, which is intended to be a wireless alternative to an existing product, to satisfy similar specifications of his current wired solution. In addition, we need specifications for the compression, wireless, and power systems, which are different from any current wired recorder system. Based on our customer's needs, we came up with the following specifications which can be seen in Figure 2 below.

	Spec #1	Spec #2	Spec #3	Spec #4	Spec #5	Spec #6
Customer Need	16 electrodes monitored	24 hr battery life	8-bit ADC resolution	>1 kHz sampling rate	Wireless transmission over 1m	Compression algorithm
Multiple channels	x					
Runtime		x				
Resolution			x	x		
Wireless					x	
Something novel						x

Fig. 2: Our Customer Needs, Converted to Design Specifications

A. Monitor Multiple Electrodes

Epilepsy monitoring demands multiple electrodes to ensure good spatial resolution. Dr. Tandon uses depth electrodes which are fine, flexible plastic electrodes attached to wires that carry currents from deep and superficial brain structures. Each plastic parent electrode has 16 recording channels on it. Therefore, our device needs have the ability to transmit data from 16 channels.

B. Long Battery Life

Our device would free patients from wires, so a long-lasting onboard battery is crucial to patients' experience. 24 hour battery life would allow patients to move around freely for a day without the need to recharge the battery.

C. ADC Resolution

Our system converts the analog data from electrodes into a digital signal. This is done by an Analog to Digital Converter (ADC). Dr. Tandon requires the ADC to have a minimum 8-bit resolution to ensure the resolution of digitized data.

D. Sampling Rate

Dr. Tandon is interested in LFP data which require a minimum of 1 kilohertz of sampling rate to prevent aliasing.

E. Wireless Transmission Range

The patient needs to be able to move around a room freely within the receiver's range. The wireless system thus should have at least a reliable transmission range of 1 meter.

F. Compression Algorithm

To add an element of novelty to our system and to be able to transmit data at higher rate, we also need to implement a compression algorithm in our system.

V. MAJOR CONCEPTS

There were three major areas of development: component selection, choice of compression algorithm, and physical design of the system. Each presented tradeoffs and ramifications for performance.

Possibly the most crucial development was the choice of components critical to each subsystem. For the interface between the electrodes and the (digital) system, we decided on the Intan Technology RHD2216 [8] as there was nothing comparable on the market. While instrumentation amplifiers aimed towards biological data are available, as are high-precision analog-to-digital converters, our team could not find any products that combined adjustable filtering, low-noise amplification, and digitization in a single QFN package. This high level of integration is greatly desirable in a system where a major goal is minimizing the total size of the circuit board, taking up roughly 64 square millimeters of space on board versus multiple chips of similar size with empty space around each and additional space taken up by traces connecting each component. A drawback of the Intan chip, however, is its high cost; this single component costs \$260, which is more than all

the other components combined plus the cost of manufacturing the prototype (just over \$200 in total).

For the wireless transmission system we chose the TI CC2652 MCU. Continuing the desire to minimize the size of the board, this component was chosen for its ability to both act as the compression MCU and wireless transceiver with its 48 MHz ARM processor operating separately from its dedicated radio controller. The CC2652 was also desirable because of its multi-standard wireless support. Our initial plan was to use Bluetooth Low Energy 5 as our transmission protocol but discovered that its layers of abstraction limited our ability to send as much neural data as we desired; due to the flexibility of the MCU we were easily able to switch to a proprietary TI protocol that provided us with the higher throughput that fit the specifications.

The goal of the power system is to not only provide a consistent system rail but also to monitor the state of the attached battery to alert the user to low power situations for recharging purposes. A 3.3V voltage regulator was chosen as all subsystems were capable of running with that supply voltage. Due to size and weight constraints our team was limited to using a 500 mAh lithium-ion battery from Illinois Capacitor, which are claimed to be the most compact Li-ion batteries on the market. For the monitoring portion of the power system we decided on a Texas Instruments system-side fuel gauge and MSP430 for the I2C interface. The fuel gauge was chosen specifically because of the system-side designation, which meant that it could be mounted on our circuit board and perform its role without having to mount a new gauge on every possible removable battery we might use with the system. Unfortunately, there were significant issues getting the gauge to properly read the remaining capacity of our batteries so due to time constraints we had to abandon integration of the fuel gauge into the final prototype. Similarly, we had planned to integrate a linear battery charger on-board the final prototype to extend runtime. However, due to delays in our battery charging board's manufacturing, we did not have time to verify the standalone charging board's performance before incorporating the charger into our final prototype. A linear charger was chosen for the battery due to the relatively low amount of charge current needed (500 mA) and the smaller footprint afforded compared to a switching charger that requires external capacitors, inductors, and pass transistors.

To ensure wireless functionality, our team used the design files for the inverted-F antenna used by TI on their CC2652 Launchpad. Direct use of the reference design with an impedance matching 50-ohm transmission line on our board gave us the best chance of a fully functional antenna system with minimal design work plus testing.

Our team decided to include compression of the neural data as a novel component of our project. However, the two different types of neural data (LFP and action potential) required different compression schemes. We tried multiple approaches to LFP compression and concluded that the best performing algorithm that ran well on our microcontroller was a simple autoregressive model where the next value is predicted using

a weighted sum of previous values, the predicted value is subtracted from the actual value, and the resulting error signal is then sent. This technique reduces the zeroth-order entropy of the signal and allows the information using fewer bits than if the full signal were transmitted. This autoregressive model provided the best results of the ones we tried, and it also was able to fit on our wireless microcontroller.

Action potential data compresses quite differently due to the fact that individual neurons fire somewhat infrequently. This lends itself well to compressive sensing, since it is likely that these data are sparse in some basis. Once the compressed data is sent to the receiver we used basis pursuit with DCT to recover the original signal. Unfortunately, this algorithm requires the use of very large matrices, and therefore was unable to fit on our wireless microcontroller. Future work on this project could include researching other wireless microcontrollers that have more RAM, so we could include action potential compression in our prototype as well.

Minimizing the size of our board was of critical importance given our goal of testing in a model animal. To this end we had a goal of producing a final prototype board that was 3 cm on a side. Due to the size of the antenna design that we used as well as the size of our transmission line this was infeasible and we ended up producing a final prototype board that was 4 cm on a side.

VI. DETAILED DESIGN AND PROTOTYPING

A. Data Collection

1) *Chip Selection:* To collect neural data, we needed an electrophysiology chip. One of the few companies that produce such chips is Intan Technologies, who is a leader in the development of specialized integrated circuits for biological sensing. Their RHD2000 series digital electrophysiology interface chips are complete low-power acquisition systems. The chip combines amplifiers, reconfigurable analog and digital filters, a 16-bit ADC and a multi-frequency electrode impedance measurement module, which makes a perfect candidate for our recording system. Our specifications require us to have a 8-bit ADC and 16 channels in collecting data. We thus picked RHD2216, a 16-channel amplifier chips with a 16-bit ADC as the core of our data acquisition system.

2) *Chip Registers and Settings:* Intan RHD2000 chips communicate using a standard SPI interface and responds to 5 basic commands: CONVERT, CALIBRATE, CLEAR, WRITE, and READ. [8]. An Intan chip functions as an SPI slave and an external SPI master device needs to configure its RAM registers upon power-up. In our system, we use a wireless chip as the SPI master and writes initialization sequences to the Intan chip. During initialization, the SPI master device sends CALIBRATE command the Intan chip, then it sends WRITE command to configure the on-chip analog filters in the low-noise amplifier to have a bandwidth range of 0.10Hz to 20kHz, the maximum range the chip can support. This filter occurs prior to digitization. Since we are interested in signals with frequencies below 500Hz, having a bandwidth upper limit of 20kHz will not affect the data acquisition result.

3) *Custom Breakout Board*: We designed a breakout board for the Intan chip, feeding it data such as square and triangle waves as well as simulated EEG data. The Intan chip then sends the digitized signals to our microcontroller via SPI protocol. The breakout board can be seen in Figure 3.

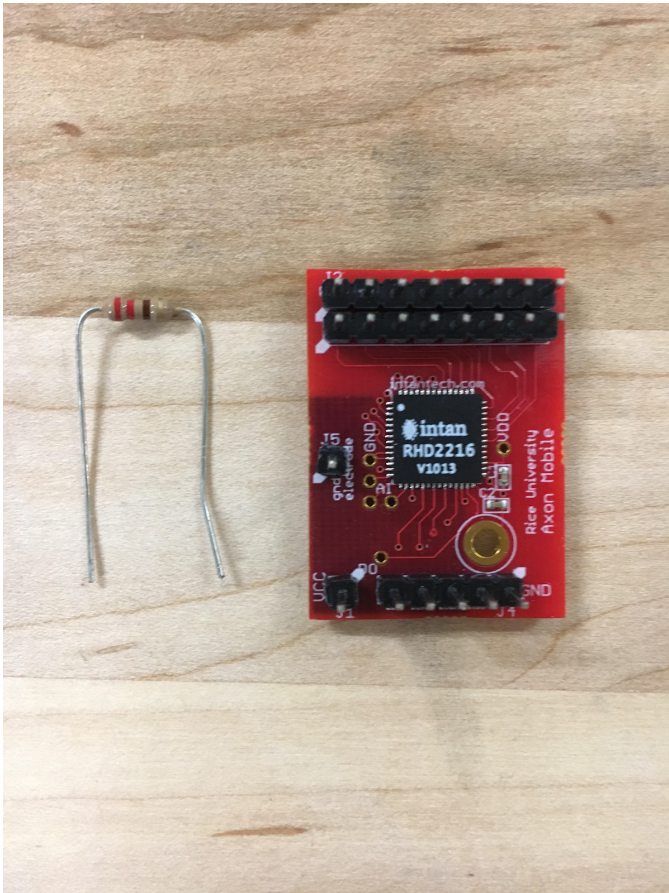


Fig. 3: Intan Chip Breakout Board (Resistor for Scale)

This board was useful in our first prototype, which consisted of the above breakout board, and two TI CC2652 Launchpads (described in the wireless section below) serving as both the transmitter and receiver in our system. It also allowed us to understand the functionality of the Intan chip before trying to implement it into a larger, full-system prototype.

B. Wireless Communication

1) Wireless Technologies: There are many types of wireless technologies available on the market and some of the most commonly used protocols are listed in Table 1 [9]–[11]. Given the requirements of transmitting data over 16 channels at a high sampling rate, we needed a wireless protocol that allows for high data throughput. WiFi, Bluetooth and Bluetooth Low Energy 5 (BLE5) are the three commonly used protocols that satisfy the data rate requirements. Among these three, BLE5 has the lowest energy consumption, which is most optimal for achieving long run time. Therefore, we initially picked BLE5 as the protocol for our wireless system.

2) Wireless Microcontroller Selection: There are a few companies on the market that produce microcontroller chips with support for BLE5. The most widely used ones are from Texas Instruments (TI), Nordic Semiconductor, Dialog Semiconductor and Cypress Semi. Due to our familiarity with TI products and close diplomatic ties with the company, we picked wireless microcontroller chips from TI for our project.

TI SimpleLink MCU platform is a product series of wireless microcontrollers [12]. Among these, CC2652 is the newest generation that support BLE5. It has 352kB flash, 80kB RAM and runs on ARM Cortex M4F core [13]. It has a maximum TX current of 7.5mA, one of the lowest in power consumption in the whole product family, which gives it the potential to run for a full day on battery power. Moreover, it has 2Mbps PHY rate on spec, which we believed would satisfy our data rate requirements.

3) BLE5 vs. Proprietary 2.4GHz: BLE5 protocol stack has many layers as shown in Figure 4, with each layers adding additional overhead to data packets. To develop a full custom BLE5 application presented a huge learning curve for us. Even though BLE5 has a Physical Layer (PHY) data rate of up to 1Mbps, the actual throughput we were able to achieve during testing was 50kbps which was below the minimum required throughput of 80kps for sampling at 250Hz from 16 channels. Moreover, TI BLE5 does not have detailed documentation for integrating the BLE library with other SPI devices which presented a huge challenge to talk to the Intan chip.

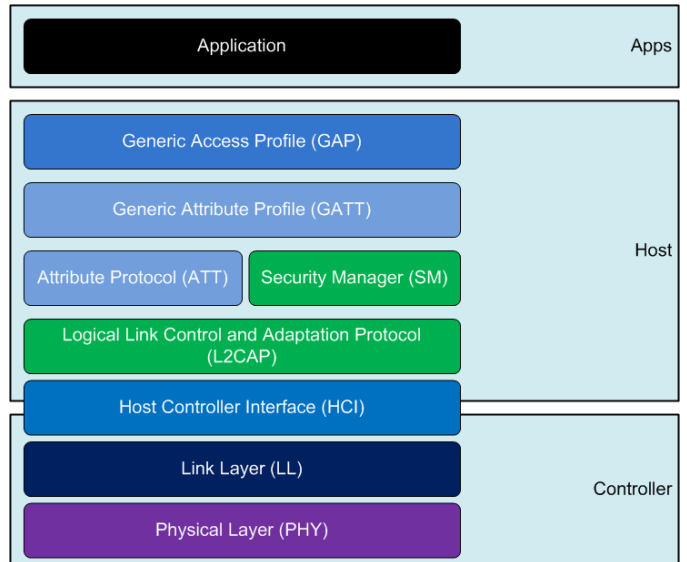


Fig. 4: Different Layers of BLE5 [14]

Given these drawbacks of the TI BLE5 library, we turned our attention to other wireless protocols CC2652 supports, Proprietary 2.4GHz RF in particular. Under this protocol, the radio controller directly accesses data from the system RAM and assembles the information bits in the packet structure as shown in Table 2. A preamble and sync word are used to synchronize transmission timing between the transmitter and receiver. The length field indicates the number of bytes in payload. To

Technology	Network Standard	Receiver Sensitivity	Max PHY Data Rate	Approx. Max Range
Wi-Fi	IEEE 802.11 b/g	-95dBm	1-54Mbps	35-110m
Bluetooth	IEEE 802.15.1	-97dBm	1-2Mbps	10m-100m
Bluetooth 5.0 (Low Energy)	IEEE 802.15.1	-95dBm	1-2Mbps	10m
ZigBee	IEEE 802.15.4	-100dBm	250kbps	10-75m
SigFox	-	-137 dBm	100bps-600bps	10-50km

TABLE I: Comparison of Common Wireless Technologies

8 bytes	32 bits	1 byte	32 bytes	16 bits
Preamble	Sync Word	Length Field	Payload	CRC

TABLE II: Data Packet Format for Proprietary 2.4GHz RF

record 16-bit data each from 16 channels, we need 32 bytes in the payload field. CRC stands for Cyclic redundancy check, which is an error-detecting code implemented by TI RF library. Proprietary 2.4GHz RF is not as complex as BLE5 and has much less overhead. Moreover, it is simpler to interweave SPI communication with radio transmission commands. Therefore, we switched to this protocol from BLE5.

4) *Wireless System Prototyping Strategy:* We knew from the very beginning that our final prototype would be a custom PCB with a data collection chip and a wireless chip onboard. To develop the wireless system, we acquired two CC2652 multi-standard wireless MCU launchpads from TI. Both devices support BLE5, Proprietary 2.4GHz, Thread and Zigbee and can talk to each other directly. They also have various serial interfaces such as SPI and UART which allow them to transmit data to a computer and other devices. We programmed one launchpad to be the transmitter and the second one to be the receiver to test the capabilities of these chips.

We started out by studying the backbone example code provided by TI to understand the workings of the protocols, then we modified the transmission code to make it transmit random data. Eventually we integrated the chip into the system by setting up SPI communication with the Intan chip and transmitting actual data.

5) *Interface with Intan Chip:* As mentioned in Section 6.2.2, the CC2652 wireless chip is the SPI master and controls the Intan chip by sending SPI commands. During initialization, the wireless chip sets the 18 internal registers on the Intan chip and requests calibration. During data acquisition period, the wireless chip sends CONVERT(C) command to read the value of voltages at channel C. To sample data from multiple channels, the wireless chip does one cycle of 16 channels to the Intan chip and collects 16-bit data from each channel.

The sampling rate is adjustable and is currently set to 380Hz for 16 channels, which is higher than the minimum sampling rate of 100Hz for extracranial EEG signals [4]. After it collects 32 bytes of data, it compresses data using compression algorithm to be introduced in Section 6.3.2. Next, the wireless packages the data into the data format shown in Table 2 and transmits data to the receiver through a 2.4GHz link. After the transmission is complete, the wireless chip continues to sample data from the Intan chip and proceeds

to next transmission.

6) *Receiver to Computer:* We are using a CC2652 evaluation board connected to a computer as the receiver. Upon receiving the data packets from the transmitter, the receiver passes the data along to the computer via UART at 921400 baud. A Python script then decodes the bit stream from UART port, displays the data change in real time and performs signal processing on the data. To ensure transceiver synchronization, we send ASCII code of “INTAN” three times in a row to the receiver at the beginning of each data transmission session. The decoding Python script discards data from UART until it detects the “INTAN” sequence, thus achieving synchronization between transceivers.

C. Data Compression

Two types of biological signals can be captured from EEG recordings. LFP signals can be captured at a sampling rate of 100 Hz and extracellular action potentials can be captured at a sampling rate of 30 kHz [4]. Because these signals significantly differ in content, shape, and quantity, we need to use a different compression mechanism for each signal type.

1) *Spike Compression:* Analysis of spike data follows a standard computational pipeline [15]. First, the signal is passed through a spike detector which either directly thresholds the signal, or thresholds a transform of the signal. The most common method for transforming is the nonlinear energy operator [16]. After spikes are identified, a time window around each detected spike is created and the spike is saved as an N-dimensional vector where N is the length of the time window. Dimensionality reduction is then performed on this set of vectors using principal component analysis (PCA) or wavelet transform. After this transform, the spikes are clustered in this reduced space using K-means clustering or density-based spatial clustering of applications with noise (DBSCAN). Since each neuron produces a unique spike morphology, this process can identify which spike came from which neuron by looking at similarities in spike morphology. Figure 5 shows an example of raw neural spikes being thresholded, windowed, and then clustered.

At the end of the process, neuroscientists only need spike times and a neuron ID since those are usually sufficient statistics for characterizing the neural signal. Because of this, many existing systems for neural recording perform spike detection and sorting locally and then export only the spike times and neuron IDs. However, there are a wide variety of adjustable parameters during spike sorting. By performing local spike sorting, researchers lose the ability to manipulate

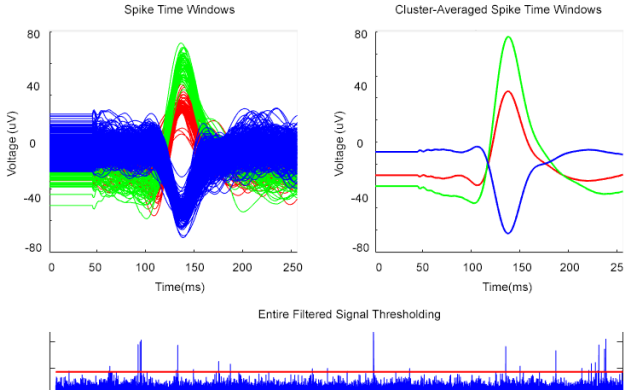


Fig. 5: Spike Sorting Clusters

the parameters to control the sorting. Saving the spike waveform before clustering is clearly a more flexible solution with minimal risk of corruption. In order to wirelessly transmit raw spikes, compression is needed due to the large amount of information communicated to the remote receiver. In order to solve this problem, we created a lossy compressive sensing algorithm that drastically reduces the amount of data that needs to be transmitted while minimally affecting the integrity of the signal. The algorithm works by first creating a Gaussian $P \times N$ (reduced sample size \times initial sample size) matrix at the receiver end and wirelessly sending that matrix to our data collection system. The data collection system then uses that Gaussian matrix to reduce the size of the signal and transmit the reduced signal to the receiver. At the receiver end, we use the random matrix with DCT orthogonal basis vectors to perform basis pursuit and transform the signal back. We tested our algorithm with data from the hc4 dataset in the CRCNS archives [17]. Post-compression signal integrity was checked using signal-to-noise and distortion ratio (SINAD). After testing out several different bases, we found that DCT performs the best on this dataset. The results of these tests are shown in Figure 6. Because we are only compressing windows of time around detected spikes, the compression rate will depend on the spike detection rate.

2) *LFP Compression*: For LFP compression, the most effective and computationally efficient approach is predictive modelling [18]. The most common form of predictive modelling is a simple autoregressive (AR) model which predicts the next value as a weighted sum of previous values of the signal. An AR(p) model is one in which the last p values of the signal are used in the prediction as follows.

$$y_t = \beta_1 y_{t_1} + \beta_2 y_{t_2} + \dots + \beta_p y_{t_p} + e$$

Historical prediction errors are used to calculate the coefficients that weight each previous observed value while e is the prediction error from the AR(p) model. During compression, the signal and coefficients are given and e needs to be calculated. During decompression, e and $y_{t_1}, y_{t_2} \dots y_{t_p}$

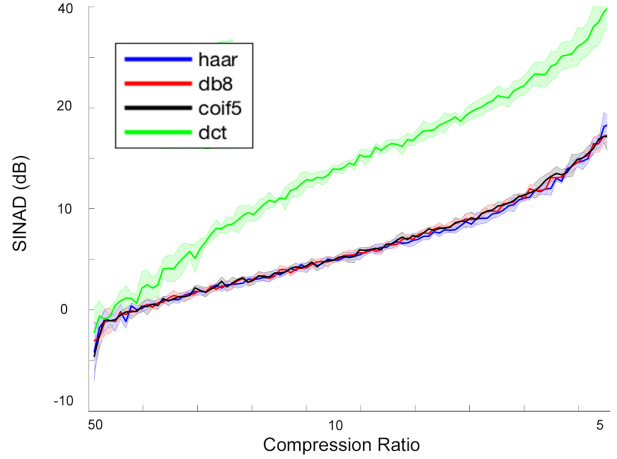


Fig. 6: Compressive Sensing Performance

are given and y_t needs to be calculated. The prediction can then be subtracted from the original signal to acquire the error signal. Since this error signal has a much lower zero-order entropy when compared to the original signal, the number of bits necessary to represent the signal is also reduced. The original signal is then perfectly reproduced at the receiver end of the system.

3) *Entire Compression System*: Although the CPU we are using is not powerful enough to support sampling at the required rate for capturing action potential data, our compression system supports both signal modalities and is depicted in Figure 7 below.

D. Power System

One of the largest constraints for the system is balancing power draw and energy storage with size and weight requirements. Given that we need a 24-hour runtime at a minimum, we have calculated the theoretical maximum worst-case current draw for our system and concluded that running the system for 24 hours continuously will take roughly 700mAh of charge; if each subsystem were to draw the maximum possible current, the wireless system would consume 13 mA [12], the Intan chip 11 mA [8], and the power system 3 mA, which corresponds to 672 mAh. Because of our weight and size limits, the largest battery we can realistically use is 500mAh, although we plan to include a battery charger on later versions of our system. With an on-board battery charger, the system can be recharged during use and extend the runtime from roughly 18 hours to indefinite, assuming consistent charging during use when low battery is indicated.

The power system is comprised of a battery, 3.3V linear regulator, “fuel gauge” IC, and microcontroller to provide a controlled system voltage as well as real-time monitoring of battery status with a visual low power indicator.

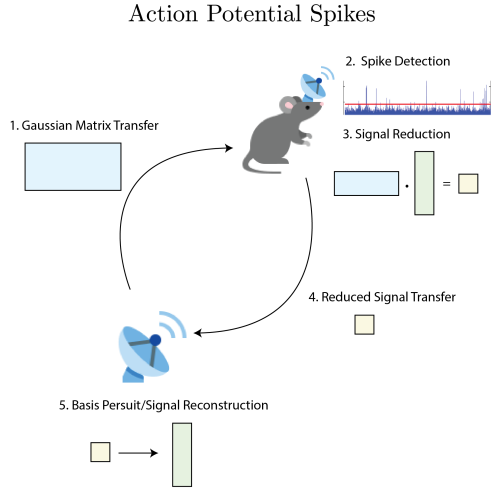


Fig. 7: Compression Flowchart for The Two Signal Modalities

E. Full Board Design

1) *Considerations for Rodent Implantation:* After achieving end-to-end functionality in our non-form-factor, discrete component prototype, we began working on a final prototype PCB, with the intent of having full functionality in rodents. Before creating this prototype, we started collaborating with Dr. Caleb Kemere's Realtime Neural Engineering Lab (RNEL) [19] so we could better understand what additional specifications our board might have to fit and how exactly the board would be placed on a rodent. We determined that our best chance for success in rodent implantation would be to design the board such that it could sit atop the rodent's head inside a plastic holder that we could design ourselves. The rodent will already have electrodes implanted in its brain and they will connect to an electrode interface board (EIB). Our board can then be connected to the EIB via a cable that we create ourselves. A diagram of this setup can be seen below in Figure 8.

This slightly complicated setup (especially the inclusion of

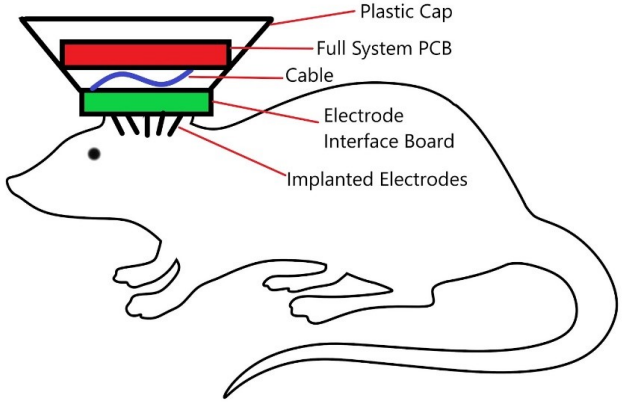


Fig. 8: Plastic Holder Containing System PCB Connected to Implanted Electrodes

a cable instead of connecting our board directly to electrodes, as it would be in future iterations) was for simplicity of implementation, as we were able to test our device on a rat that was already being used for experimentation. This rat already had implanted electrodes and an EIB on the top of his head, so we designed our boards specifically to be connected to the EIB on this rat. Since we knew which rat we would be testing on, we needed the final prototype to be under 50 grams (including the board, the plastic holder, the cable, and the battery), as the rat we used weighed 500 grams and it is standard practice to not put more than 10% of a rodent's body weight on its head. It was also important for the board to be at most 4x4 centimeters in size.

2) *First Iteration of Full Board:* We decided to create a non-form-factor version of the final board first before creating the board that would be implemented on a rodent. This was so we could verify that all of our ICs worked together appropriately and our transmission line/antenna functioned correctly before we concerned ourselves with getting the prototype down to 4x4 centimeters. Thus, we created the 6x6 centimeter board seen below in Figure 9.

This board has four layers with all components placed on the top layer, and three different ground layers. We structured it this way because of the need to separate the ground planes of the digital components (the ICs and their associated passive components) and RF components (the antenna and the passives along the analog transmission line). The second layer contains a ground plane that only covers the analog components, and the third and fourth layers are ground planes for the digital components. We chose a four-layer board over a two-layer board because the 4-layer board had a thinner substrate between copper layers, which allowed us to more easily match the impedance on all the RF traces. Two-layer boards have a thicker substrate and in order to have impedance matching, we would have needed traces so thick they completely overshadowed the passive components the traces touched. With a four-layer board, we only needed 17mil traces, which was manageable.

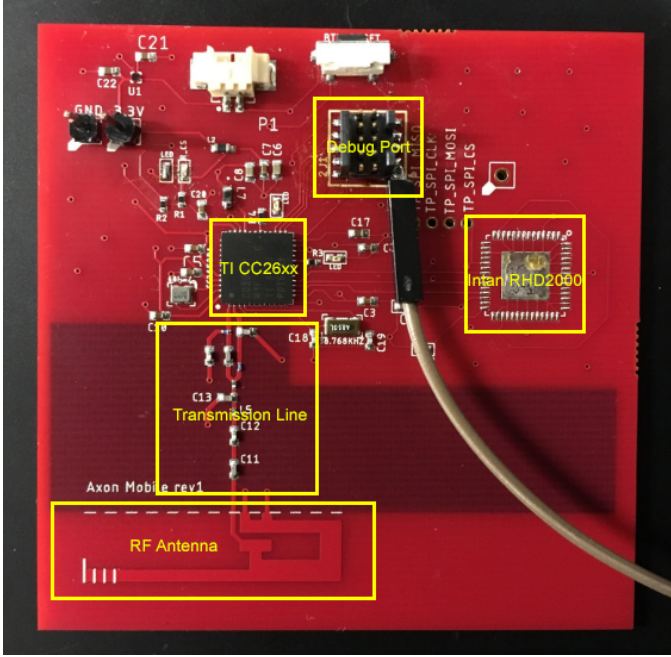


Fig. 9: First Iteration of Full-System Prototype

This board consists of two main ICs: our Intan chip and the microcontroller we are using for wireless communication. The latter also has our code for LFP data compression implemented on it. The PCB also has an integrated inverted F antenna for transmitting data. The antenna and the transmission line match those of the TI CC2652 Launchpad from our discrete-subsystem prototype almost exactly, as we knew that system worked and therefore wanted ours to be as similar as possible.

Because Intan chips are so expensive, we opted to not place an Intan chip on this board, and instead connected our Intan breakout board for testing purposes. We also tested the board by itself by sending noise from the floating pins, as a proof of concept that the wireless components of this prototype were functioning.

3) Second Iteration of Full Board (Final Prototype): After verifying that the 6x6 centimeter board was functioning, we designed our final prototype, which is form-factor and was designed with our rat-implementation dreams in mind. This board can be seen below in Figure 10.

The final prototype is 4x4 centimeters in size, as desired. It is also four layers, for the same reason as the 6x6 centimeter board – we needed separate ground planes for the analog and digital components, and four layers also provided a thin enough substrate between copper layers in order to reasonably implement impedance matching in the transmission line.

The Intan chip was obviously included in this prototype. We also added header pins for the electrodes because this was the simplest way for us to ensure our board could be used on a rat in Dr. Kemere's lab; we weren't positive what sort of connectors the EIB used, so this way a simple cable could be soldered to interface between the EIB and our board. In a future iteration, we would cut out the need for a cable and

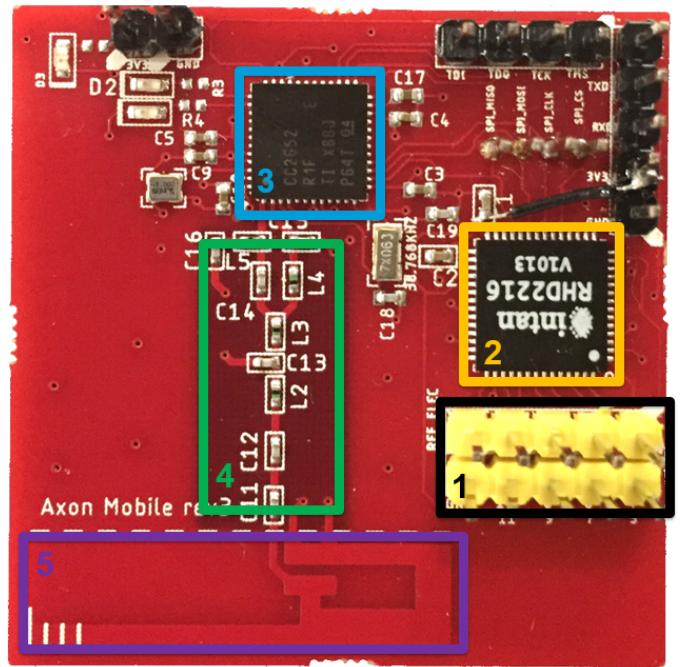


Fig. 10: Final Prototype PCB. (1) Electrode Interface Pins; (2) Intan Chip for Neural Data Collection and Pre-Processing; (3) CC2652 Wireless Chip; (4) Transmission Line; (5) Inverted F Antenna

include the correct connectors. This would also cut down on size and weight, as the current header pins are much larger than necessary. To keep the final prototype as small as possible, we removed the debugging port (seen in Figure 9) and opted for header pins that could be configured along the border of the final prototype so they would take up less space. We also removed other items, such as the reset switch, that were present in the 6x6 centimeter board simply because they were part of the CC2652 Launchpad but had no purpose in our specific design.

We also made the decision to have the digital components extend vertically into the region of the transmission line (the board in Figure 9 keeps all digital components above the transmission line). We originally wanted to keep the digital and analog parts of this board as far apart as possible to minimize interference, but realized we would be unable to fit the board in a 4x4 centimeter space without having them overlap by some amount. We still kept the separate ground planes, and the transmission line is as straight as possible (and matches the CC2652 Launchpad schematic exactly).

VII. TESTS AND RESULTS

A. Full System Input/Output Testing

To test our system end-to-end, we wrote a Labview program that converts existing ECoG data to analog voltages that we can send to our Intan chip to be sampled, and then sent to our wireless microcontroller to be transmitted. We were successful

in receiving simulated EEG data; a depiction of the transmitted and received data can be seen below in Figure 11.

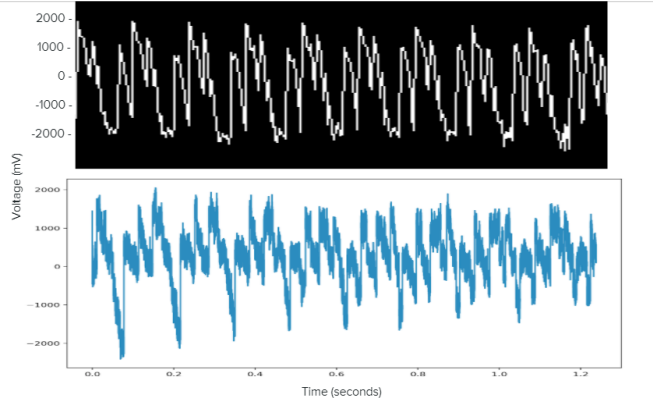


Fig. 11: (Top) Simulated EEG Data Sent to Intan Chip from Labview Program; (Bottom) Received EEG Data From Wireless Microcontroller Plotted in MATLAB

This test was using only one channel, and we were able to sample at 1 kHz. As shown in Figure 3 from the Wireless Communication section, we can successfully transmit from two channels at our desired ECoG sampling frequency. If we want to transmit data from all 16 channels on the Intan chip, we can still sample the data at 390 Hz, which is greater than the typical sampling rate for EEG signals [20]. Additionally, we can receive transmitted data from over 10 meters away, which is much greater than our spec of a 1 meter transmission range.

B. Wireless System Testing Data Transmission Testing

We measured the sampling using a logic analyzer hooked up to the SPI pins of the CC2652 chip. Data acquisition and transmission took turns to use the CPU as shown in Figure 12. MISO channel shows the data received by the wireless chip during data acquisition. The blank period between neighboring data acquisition period is when the wireless chip packages the data and transmits to the receiver.

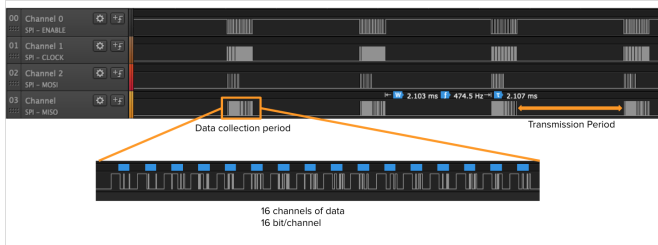


Fig. 12: Sampling Rate Measurement with Logic Analyzer

We were able to achieve a throughput of 103kbps for 16 channels at a sampling rate of 390Hz. Higher sampling rate is achievable for fewer channels as shown in Figure 13. 1 kHz sampling rate was achievable for 2 channels which gave us the capability to transmit LFP data.

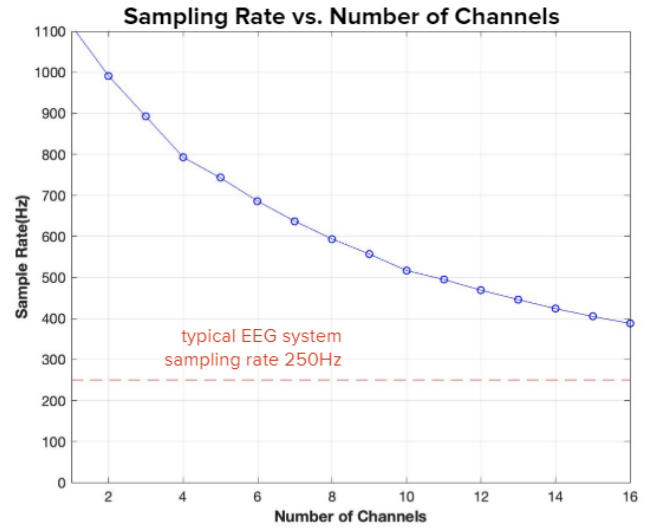


Fig. 13: Sampling Rate vs. Number of Channels Sampled

C. Wireless System Range Testing

TI offers some wireless system testing softwares such as SmartRF Studio. We verified the functionality of our custom board by connecting it to SmartRF Studio. Then we control the CC2652 chip on our custom board to send test sequences to the receiver launchpad. SmartRF Studio is able to measure received signal strength indicator (RSSI) value, which is a measurement of power present in the received radio signal. While CC2652 chip has a maximum receiver sensitivity of -103dBm [12], an RSSI value greater than -75 dBm is a general indication of a sufficiently strong signal.

We moved the transmitter away from the receiver slowly and observed the RSSI reading on the receiver as shown in Figure 14. When the transmitter and receiver were placed side by side to each other, we registered an RSSI reading of -32dBm, indicating a strong signal. As we moved the transmitter away, the RSSI value began to fall, reaching around -58dBm at 5m away and -74dBm at 10m away. The RSSI value at 10m was higher than the good signal strength cutoff and well within the range of receiver sensitivity. Therefore, we concluded that our wireless system has a reliable range of 10m.

D. Full System Power Testing

Using a Keithley 2400 source meter we measured the current draw of the final prototype over 30 minutes to allow for an accurate average of power consumption. The current draw was always within 1 mA of 25.5 mA which, for the 500 mA battery used in the system, translates to 19.6 hours of runtime. While short of our planned 24 hour runtime, this is constrained by both the weight and size limits of our battery as well as the specific current draws of the other subsystems, most notably the Intan chip and wireless MCU.

E. Extracranial EEG Testing

For demonstration with humans, we used an OpenBCI Ultracortex Mark IV EEG headset that could attach our board

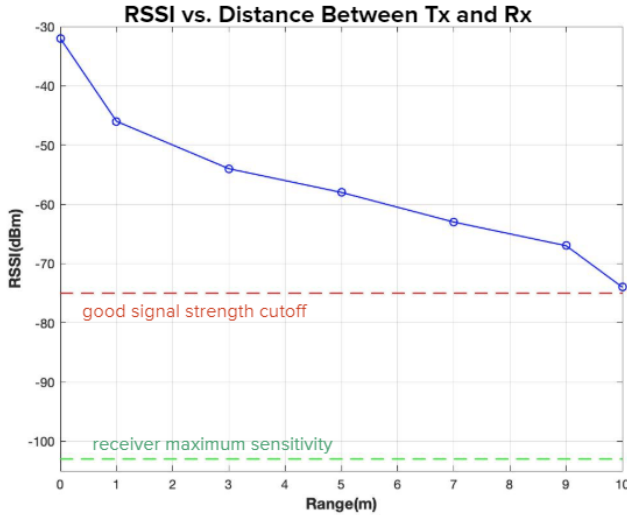


Fig. 14: RSSI vs. Distance Between Transmitter and Receiver(m)

to the back of and record neural data in an extracranial manner (seen in Figure 15 below). OpenBCI provided the cables, comfort nodes, 2 flat electrodes, 6 spiky electrodes, and an ear clip wire while the headset frame was 3-D printed by a local company. Once the sender and receiver chips are in communication, utilizing the cap for data collection is done by first connecting the electrode wires to the board's header pins as well as connecting the ear clip wire to the reference pin. Putting on the headset and attaching the ear clip to the user's ear lobe produces instant results for display.

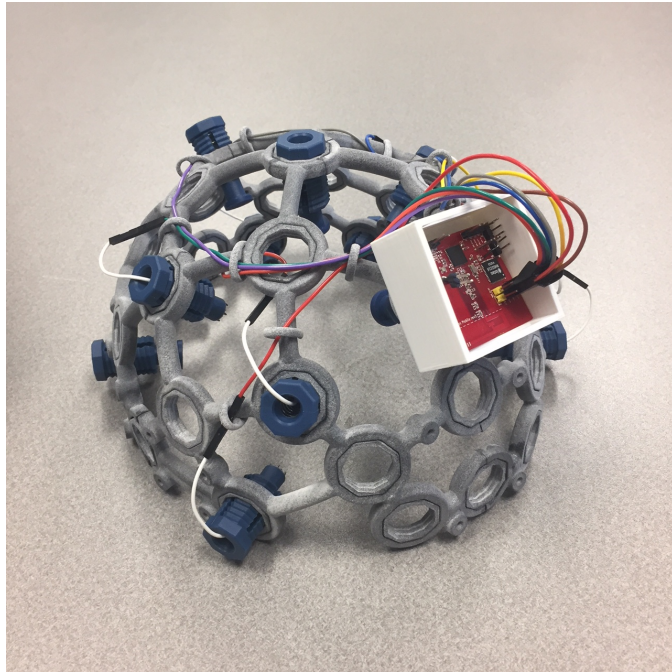


Fig. 15: 3D Printed EEG Headset

To better attach our device to the headset, we 3-D printed

a special holder for the board that can be screwed through one of the open holes in the back of the headset. This allows the device to sit more securely and minimizes the risk of the board slipping away and dangling precariously by its wires.

F. Intracranial EEG Testing

We collaborated with Dr. Caleb Kemere's Realtime Neural Engineering Lab (RNEL) to acquire a rat for intracranial testing. As Dr. Kemere's lab was already experimenting with rat neural data, we were able to simply swap their wired system with our wireless one. The rat that we used already had a set of connection ports implanted through the skull that we could plug our system into after creating a cable to connect the two. In addition, we 3-D printed a headstage to house the device and battery as it sits on top of the rat's head. The battery, board, cable, and case combine to weigh about 45 grams, which is just light enough for the rat to walk around and not be weighed down. A photo of the rat with our device on his head can be seen below in Figure 16.



Fig. 16: Neural Recording Device Connected to Rat's Brain (The pink material on top of the rat's head is dental acrylic, commonly used in dentures)

Upon attaching our device to the connections on the rat's head, the receiver started collecting data, which could be displayed on the laptop it was connected to. At that point, the rat was able to freely move about its enclosure as the device collected data. The way the device was connected allowed for 4 channels of data to be collected simultaneously. A snippet of this data can be seen below in Figure 17.

The rat and the receiver were each in separate rooms as the data was transmitting, which stood as a testament to the range of the device. Since we were dealing with live animals, all work with vertebrate subjects were approved by the Rice IACUC.

VIII. CONCLUSION

Our wireless neural recorder is scalable for operation in humans, and potentially modular so the number of EEG recording chips/electrodes is customizable. The creation of

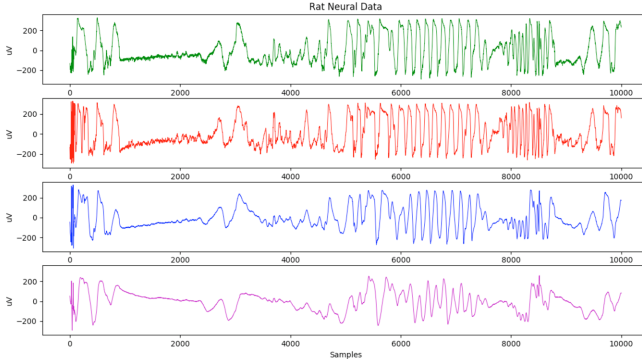


Fig. 17: Collected Rat Neural Data; Transmitted Wirelessly Through Four Channels

a wireless neural recorder that is fully functional when implanted in rats will open the door for future research on efficient wireless transmission of neural data, and will also provide a stepping stone towards implementing such a device in humans.

REFERENCES

- [1] World Health Organization, “Epilepsy,” www.who.int, Feb. 7, 2019. [Online]. Available: <https://www.who.int/news-room/fact-sheets/detail/epilepsy>. [Accessed: Feb. 20, 2019].
- [2] K. Hashiguchi, et al, “Correlation between scalp-recorded electroencephalographic and electrocorticographic activities during ictal period” *Seizure: European Journal of Epilepsy*, vol. 20, no. 3, pp. 238-247, April 2007. [Online]. Available: <https://www.seizure-journal.com/article/S1059-1311%2806%2900248-2/fulltext>. [Accessed Feb. 20, 2019].
- [3] D. E. Carlson, J. S. Borg, K. Dzirasa, L. Carin, “On The Relationship Between LFP & Spiking Data,” *Advances in neural information processing systems*, vol. 3, pp. 2060-2068, January 2014. [Online]. Available: <http://people.ee.duke.edu/~lcarin/LFPPandSpiking.pdf>. [Accessed Feb. 28, 2019].
- [4] F. Chen, A. P. Chandrakasan, V. Stojanovi, “A signal-agnostic compressed sensing acquisition system for wireless and implantable sensors,” in *IEEE Custom Integrated Circuits Conference*, 2010, San Jose, CA, USA [Online]. Available: IEEE Xplore, <https://ieeexplore.ieee.org/stamp/stamp.jsp?tp=&arnumber=5617383&tag=1>. [Accessed: Feb. 28, 2019].
- [5] N. Tandon of The University of Texas Health Science Center at Houston, “The Neuroimaging and Electrophysiology Lab.” [Online]. Available: <http://www.tandonlab.org/>. [Accessed: Feb. 28, 2019].
- [6] Medtronic, “Activa PC Neurostimulator,” April 2017. [Online]. Available: <https://www.medtronic.com/us-en/patients/treatments-therapies/neurostimulator-dystonia/activa-pc.html>. [Accessed: Feb. 28, 2019].
- [7] Blackrock Microsystems, “NeuroPort System,” 2018. [Online]. Available: <https://blackrockmicro.com/neuroscience-research-products/neural-data-acquisition-systems/neuroport-daq-system/>. [Accessed: Feb. 28, 2019].
- [8] Intan Technologies, “RHD2000 series digital electrophysiology interface chips,” 2019. [Online]. Available: <http://intantech.com/products-RHD2000.html>. [Accessed: Feb. 28, 2019].
- [9] Al-Kashoash, Hayder & Kemp, Andrew. (2017). “Comparison of 6LoWPAN and LPWAN for the Internet of Things”. *Australian Journal of Electrical and Electronics Engineering*. 10.1080/1448837X.2017.1409920.
- [10] Spons, Jon Gunnar. “Things You Should Know About Bluetooth Range.” Nordic Semiconductors [Online]. Available: <https://blog.nordicsemi.com/getconnected/things-you-should-know-about-bluetooth-range>. [Accessed: Apr. 29, 2019]
- [11] Pietrosemoli, E. (n.d.). “Wireless standards for IoT.” [Online]. Available: http://wireless.ictp.it/school_2019/slides/WirelessstandardsforIoT.pdf. [Accessed: April 29, 2019]
- [12] Texas Instruments, “CC2652 SimpleLink Multiprotocol 2.4-GHz Wireless MCU,” 2019. [Online]. Available: <http://www.ti.com/lit/ds/symlink/CC2652.pdf>. [Accessed: Feb. 28, 2019]
- [13] Texas Instruments, “Bluetooth Low Energy - products.” [Online]. Available: <http://www.ti.com/wireless-connectivity/simplelink-solutions/bluetooth-low-energy/products.html>. [Accessed: Apr. 29, 2019]
- [14] Texas Instruments, “Bluetooth Low Energy Scanning and Advertising.” [Online]. Available: http://dev.ti.com/tirex/content/simplelink_academy_cc2640r2sdk_2_40_03_00/modules/blestack/ble_scan_adv_basic/ble_scan_adv_basic.html. [Accessed: Apr. 29, 2019]
- [15] M. Lewicki, “A review of methods for spike sorting: the detection and classification of neural action potentials,” *Network: Computation in Neural Systems*, vol. 9, no. 4, pp. R53-R78, July 1998. [Online]. Available: https://www.tandfonline.com/doi/pdf/10.1088/0954-898X_9_4_001?needAccess=true. [Accessed: Feb. 28, 2019].
- [16] P. Maragos, J. F. Kaiser, and T. F. Quatieri, “On amplitude and frequency demodulation using energy operators,” *IEEE Trans. Signal Processing*, vol. 41, pp. 1532-1550, Apr. 1993. [Online]. Available: <https://ieeexplore.ieee.org/document/212729>. [Accessed: Feb. 28, 2019].
- [17] K. Mizuseki, et al, “Extracellular recordings from multi-site silicon probes used for clustering of neuron responses in rat hippocampal and entorhinal regions,” 2014. [Online]. Available: CRCNS.org. [Accessed: Feb. 28, 2019].
- [18] J. Cinkler, X. Kong, N. D. Memon, “Lossless and Near-lossless Compression of EEG signals,” in *Conference Record of the Thirty-First Asilomar Conference on Signals, Systems and Computers*, 2-5 Nov. 1997, Pacific Grove, CA, USA [Online]. Available: IEEE Xplore, <https://ieeexplore.ieee.org/abstract/document/679140>. [Accessed: Feb. 28, 2019].
- [19] C. Kemere of Rice University, “Realtime Neural Engineering Lab (RNEL).” [Online]. Available: <https://rnel.rice.edu/>. [Accessed: Feb. 28, 2019].
- [20] American Clinical Neurophysiology Society, “Guidelines for Recording Clinical EEG on Digital Media,” 2006. [Online]. Available <https://www.acns.org/pdf/guidelines/Guideline-8.pdf>. [Accessed: Feb. 28, 2019]